# HST Images of Twenty Nearby Luminous Quasars

John N. Bahcall[1], Sofia Kirhakos[1], and Donald P. Schneider[2]

[1] Institute for Advanced Study, School of Natural Sciences, Princeton, NJ 08540, USA
[2] Department of Astronomy and Astrophysics, The Pennsylvania State University, University Park, PA 16802, USA

**Abstract.** We present observations with the Hubble Space Telescope for a representative sample of 20 intrinsically luminous quasars with redshifts smaller than 0.30. These observations show that luminous quasars occur in diverse environments, including ultra-luminous ellipticals, normal ellipticals, spirals with H II regions, complex systems of gravitationally interacting components, and faint nebulosity. The quasar host galaxies are centered on the quasar to the accuracy of our measurements, 400 pc. Contrary to expectations, there are more radio quiet quasars in ellipticals than in spirals. Most of the radio loud quasars are, as expected, in ellipticals. These 20 luminous quasars occur preferentially in galaxies that are more luminous than the typical field galaxies. Eight companion galaxies lie within projected distances of 10 kpc from the quasar nuclei.

## 1 Observations and the Unprocessed Data

To study the nature of the environment of quasars, we have observed a sample of 20 of the most luminous ($M_V < -22.9$, for $H_0 = 100$ km s$^{-1}$ Mpc$^{-1}$, $\Omega_0 = 1.0$) nearby ($z < 0.30$) radio-quiet and radio-loud quasars, using the Wide Field Camera (WFPC2) of the Hubble Space Telescope (HST). The quasar images were placed at the center of WF3 and the visual-band filter F606W was selected for its high throughput. The size of WF3 is $800 \times 800$ pixels and its image scale is $0\farcs0996$ pixel$^{-1}$.

Figure 1 shows images of eleven of the 20 quasars, plus the image of a blue star (upper left-hand panel) for comparison. The only image processing performed on these images is cosmic ray removal and pipeline STScI flatfielding. The exposure times for the quasar images are 1100 s or 1400 s. The exposure time of the star image shown is 20 s, which yields a total number of counts similar to that obtained in the quasar images. The star is MMJ 6490 in the M67 cluster. Its apparent $V$ magnitude is 10.99 and its $B - V = 0.11$ (Montgomery, Marschall & Janes 1993). As can be seen in Figure 1, some of the quasars are noticeably non-stellar, and features of host galaxies are visible in the unprocessed *HST* images. In some cases, like NAB 0205+02, PG 0953+414, and PG 1307+085, it is difficult to distinguish the quasar image from the star.

## 2 Subtraction of a Stellar Point-Spread Function

We have observed four blue stars in the M67 cluster to use as point-spread function (PSF); the calibration stars (and their $B-V$ colors) are: MMJ 6481($-0.073$), MMJ 6490(0.11), MMJ 6504(0.22), and MMJ 6511(0.34). Their apparent magnitudes range from $V = 10.03$ to $V = 10.99$. For each star, a series of four images were used by Krist and Burrows (1996) to produce a PSF that samples the full dynamic range of the star image and covers the saturation range found in the quasar images.

We subtracted all four PSFs determined by Krist and Burrows from each of the quasars, and then selected the result that gave the cleanest subtraction.

We fit a stellar point-spread function to each quasar image and subtracted a multiple of the normalized PSF to search for underlying diffuse light from hosts. The quasar images with the PSF subtracted presented were obtained by minimizing the $\chi^2$ in unsaturated annular regions (typical inner and outer radii of $1''$ and $3''$), centered on the quasar. Adjustments of the amount of PSF subtraction were often made after visual inspection of the "best-fit" PSF-subtracted images.

Figure 2 shows the images for all the quasars in our sample after a best-fit stellar point-spread function (PSF) was subtracted from the original images, many of which are shown in Figure 1.

## 3 Methods of Analysis

We have used three different methods of analysis to determine the properties of the 20 quasar hosts.

### 3.1 Aperture Photometry

We performed aperture photometry in circular annuli centered on the quasars, after a best-fit PSF was subtracted. An inner radius of $r = 1.0''$ was used for all quasars, except for HE 1029$-$140 and 3C 273. In most observations, the region $r < 1''$ is contaminated by artifacts left by the PSF subtraction. The saturated areas in the images of HE 1029$-$140 and 3C 273 are larger; for those two cases, the inner radii used were $1.5''$ and $2.0''$, respectively. The outer radii chosen in general represent how far we could see the host galaxy.

### 3.2 One-Dimensional Radial Profiles

The one-dimensional azimuthally-averaged surface brightness profiles of the host galaxies were constructed from the *HST* data after subtraction of a best-fit stellar PSF. Regions affected by saturation, diffraction spikes, or residual artifacts from the PSF subtraction were not included in the azimuthally averaged profiles. For each galaxy, we obtained a best-fitting exponential disk (henceforth Disk) and a de Vaucouleurs (1948, henceforth GdV) profile that fits the observed data in the region $r \geq 1''$.

### 3.3 Two-Dimensional Fit

The *HST* imaging provides greater detail than has been available previously in ground-based images of luminous quasars. Traditionally, the properties of host galaxies have been determined in ground-based studies by making model fits to azimuthally-averaged radial profiles.

To take advantage of the *HST* resolution, we have developed software to fit a two-dimensional model to the PSF-subtracted quasar images. For each quasar, we fit an analytic galaxy model (exponential disk or de Vaucouleurs profile) to the data. The area used for the fit was approximately an annular region, centered on the quasar, that excluded the central area ($r < 1.0''$), and the remnants of the diffraction spikes or other artifacts clearly due to improper PSF subtraction. We fit four parameters: the (x,y) pixel position of the center, the total number of counts, and the radius (effective radius or scale length) in the galaxy model.

## 4 Magnitude of the Host Galaxies

Table 1 lists our best estimates for the magnitudes of the host galaxies in our sample; these magnitudes were obtained by fitting a two-dimensional analytic galaxy model to the data. We also list the effective radius or exponential scale length, and give the morphology of the host based on visual inspection of the images.

A difference between aperture and model magnitudes is expected because the aperture magnitudes do not include the area within 1" of the quasar; all of the models we considered have surface brightnesses that increase monotonically toward the center.

The two-dimensional models are somewhat fainter than the corresponding one dimensional fits. Specially, we find:

$$\langle m_{606\mathrm{W},2-\mathrm{D}} - m_{606\mathrm{W},1-\mathrm{D}} \rangle = \begin{cases} 0.4 \pm 0.2, & \mathrm{GdV} \\ 0.3 \pm 0.1, & \mathrm{Disk} \end{cases} . \tag{1}$$

Similarly, the magnitudes of the hostphotome galaxies estimated by fitting a GdV model to the azimuthal averaged radial profile of the residual light are on average 1.0 mag brighter than the magnitudes obtained from aperture photometry; fitting an exponential disk model gives magnitudes that are on average 0.5 brighter than the results from aperture photometry:

$$\langle m_{606\mathrm{W},1-\mathrm{D}} - m_{606\mathrm{W},\mathrm{aperture}} \rangle = \begin{cases} -1.1 \pm 0.2, & \mathrm{GdV} \\ -0.4 \pm 0.2, & \mathrm{Disk} \end{cases} . \tag{2}$$

For the two-dimensional model fits, we have on average

$$\langle m_{606\mathrm{W},2-\mathrm{D}} - m_{606\mathrm{W},\mathrm{aperture}} \rangle = \begin{cases} -0.7 \pm 0.2, & \mathrm{GdV} \\ -0.2 \pm 0.1, & \mathrm{Disk} \end{cases} . \tag{3}$$

The 2-D (1-D) GdV model gives magnitudes for the host that are on average 0.6 mag (0.5 mag) brighter than the exponential disk estimates.

The results from the two-dimensional fits indicate that the host galaxies are typically centered within 400 pc of the location of the quasar point source.

**Table 1.** Magnitudes and Morphology for Quasar Host Galaxies

| | | Two−Dimensional | | | |
|---|---|---|---|---|---|
| Object | $z$ | $m_{606}$ | $M_V^b$ | $r('')^a$ | Morphology |
| PG 0052+251 | 0.155 | 17.2 | −20.9 | 1.3 | Sb |
| PHL 909 | 0.171 | 17.2 | −21.0 | 2.3 | E4 |
| NAB 0205+02 | 0.155 | 19.0 | −19.1 | 0.7 | S0? |
| 0316−346 | 0.265 | 18.3 | −20.8 | 1.2 | Inter. |
| PG 0923+201 | 0.190 | 17.5 | −21.0 | 2.9 | E1 |
| PG 0953+414 | 0.239 | 18.8 | −20.2 | 1.1 | ? |
| PKS 1004+130 | 0.240 | 16.9 | −22.0 | 1.2 | E2 |
| PG 1012+008 | 0.185 | 17.7 | −20.7 | 1.6 | Inter. |
| HE 1029−140 | 0.086 | 16.2 | −20.5 | 3.2 | E1 |
| PG 1116+215 | 0.177 | 16.9 | −21.4 | 1.4 | E2 |
| PG 1202+281 | 0.165 | 17.7 | −20.5 | 1.4 | E1 |
| 3C 273 | 0.158 | 16.0 | −22.1 | 3.7 | E4 |
| PKS 1302−102 | 0.286 | 18.2 | −21.1 | 1.1 | E4? |
| PG 1307+085 | 0.155 | 17.8 | −20.2 | 1.3 | E1? |
| PG 1309+355 | 0.184 | 17.3 | −21.1 | 1.2 | Sab |
| PG 1402+261 | 0.164 | 18.3 | −19.9 | 1.6 | SBb |
| PG 1444+407 | 0.267 | 18.4 | −20.5 | 1.0 | E1? |
| 3C 323.1 | 0.266 | 18.1 | −21.0 | 1.6 | E3? |
| PKS 2135−147 | 0.200 | 17.4 | −21.1 | 2.6 | E1 |
| PKS 2349−014 | 0.173 | 16.2 | −22.1 | 4.8 | Inter. |

[a] Effective radius or exponential scale length.
[b] (F606−$V$) from Fukugita *et al.* (1995).

## 5 Summary

The most luminous nearby quasars exist in a variety of environments. There are three hosts that apparently are normal spirals with H II regions (PG 0052+251, PG 1309+355, and PG 1402+261), seven ellipticals (PHL 909, PG 0923+201, PKS 1004+130, HE 1029−140, PG 1116+215, 3C 273, and PKS 2135−147), as well as three obvious cases of current gravitational interaction (0316−346, PG 1012+008, and PKS 2349−014). There are also five other hosts that appear to be elliptical galaxies and are listed as En(?) in Table 1. The hosts for two of the quasars (NAB 0205+02 and PG 0953+414) are faint and difficult to classify.

There are more radio quiet quasars in galaxies that appear to be ellipticals than in spiral hosts, contrary to expectations. However, the HST images con-

firmed the expectations based upon ground-based observations that nearly all radio loud luminous quasars occur in elliptical galaxies.

The *HST* images frequently reveal companion galaxies that are projected very close to the quasar, in some cases as close as $1''$ or $2''$. We found 20 galaxy companions that are projected closer than 25 kpc to the center-of-light of a quasar and brighter than $M_($F606W$) = -16.4$. The amplitude for the quasar-galaxy correlation function determined from our data is $3.8 \pm 0.8$ times larger than the galaxy-galaxy correlation function (Fisher *et al.* 1996).

Our results are inconsistent with the hosts having a Schechter luminosity function. The average absolute magnitude for a field galaxy is about 1.8 mag fainter than $M_V(L^*) = -20.5$ (for an assumed minimum luminosity of $M_V(L^*) = -17$; see, e. g., Efstathiou, Ellis,& Peterson 1988 for a discussion of the field galaxy luminosity function). In our sample (see Table 1) the average host is $M_V(L^*) = -20.9$. We conclude that on average, the host galaxies of the luminous quasars in our sample are about 2.2 magnitudes more luminous than typical field galaxies.

The presence of very close companions, the images of current gravitational interactions, and the higher density of galaxies around the quasars suggests that gravitational interaction plays an important role in triggering the quasar phenomenon. Details of the observations, data analysis, and results of this program can be found in Bahcall, Kirhakos and Schneider (1995, 1996) and Bahcall *et al.* (1997).

For electronic versions of the images and papers discussing individual objects, see: http://www.sns.ias.edu/~jnb.

## References

Bahcall, J. N., Kirhakos, S., & Schneider, D. P. (1995): *ApJ*, **447**, L1
Bahcall, J. N., Kirhakos, S., & Schneider, D. P. (1996): *ApJ*, **457**, 557
Bahcall, J. N., Kirhakos, S., Schneider, D. P., & Saxe, D. H. (1997): to appear in *ApJ*, **479**, April 20
de Vaucouleurs, G. (1948): *Ann. d'Ap.*, **11**, 247
Efstathiou, G., Ellis, R. S., & Peterson, B. A. (1988): *MNRAS*, **232**, 431
Fisher, K. B., Bahcall, J. N., Kirhakos, S., & Schneider, D. P. (1996): *ApJ*, **468**, 469
Montgomery, K. A., Marschall, L. A., & Janes, K. A. (1993): *AJ*, **106**, 181

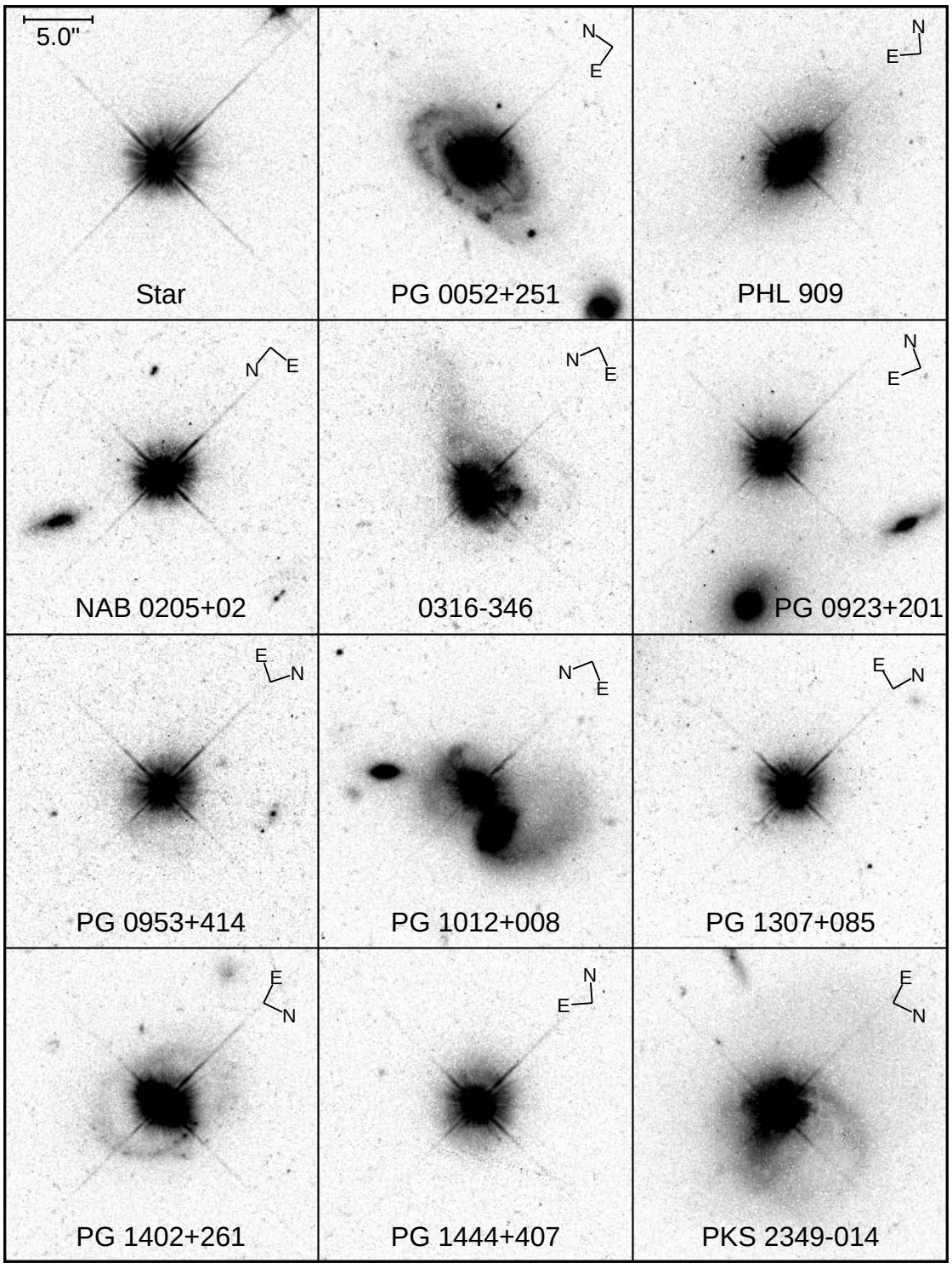


**Fig. 1.** Unprocessed *HST* images of 11 luminous nearby quasars and a blue star for comparison (upper left-hand panel). Each image is $23'' \times 23''$.

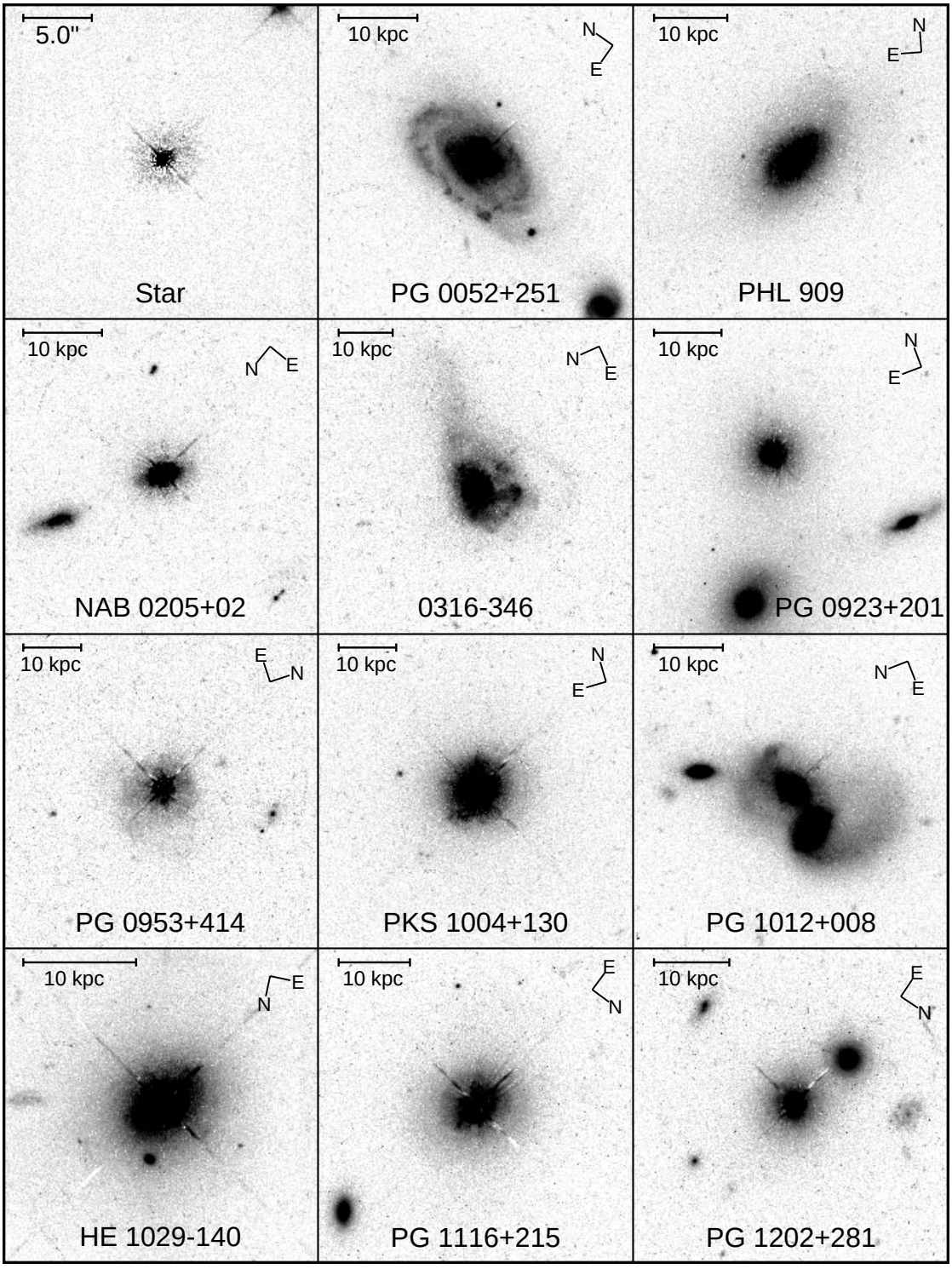


**Fig. 2.** *HST* images of 20 luminous nearby quasars and a blue star for comparison (upper left-hand panel), with a best-fit PSF for a standard blue star subtracted. Each image is $23'' \times 23''$.

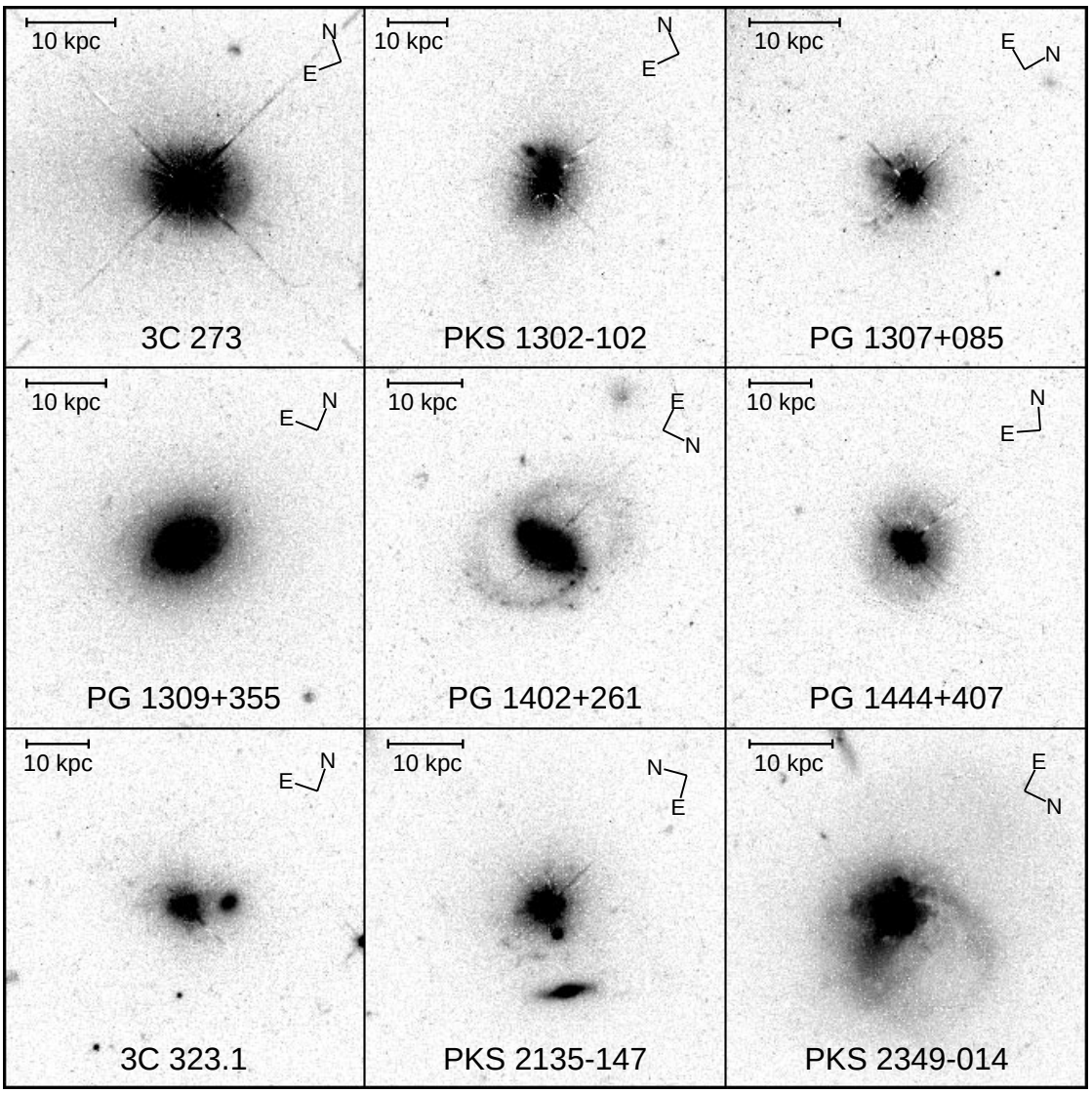


**Fig. 2.** *Continued.*